Biochimica et Biophysica Acta 1808 (2011) 127–139

Contents lists available at ScienceDirect

Biochimica et Biophysica Acta

journal homepage: www.elsevier.com/locate/bbamem

NMR evidence of GM1-induced conformational change of Substance P using isotropic bicelles

Anindita Gayen [a], Sudipto Kishore Goswami [b], Chaitali Mukhopadhyay [a,*]

[a] Department of Chemistry, University of Calcutta, 92 APC Road, Kolkata 700009, India
[b] NMR Application Chemist, Bruker India Scientific Private Limited, 22 B Ruby Park South, Kolkata 700078, India

ARTICLE INFO

Article history:
Received 16 April 2010
Received in revised form 24 August 2010
Accepted 22 September 2010
Available online 16 October 2010

Keywords:
Substance P
NK_1R
NMR
GM1
Bicelle

ABSTRACT

Substance P (SP) is one of the target neurotransmitters associated with diseases related to chronic inflammation, pain and depression. The selective receptor for SP, NK_1R is located in the heterogeneous microdomains or caveolae in membrane. Gangliosides, specifically GM1, are markers of these heterogeneous sites. Also, gangliosides are considered as important regulatory elements in cell–cell recognition and cell signaling. In the present work, we describe the conformations of Substance P in the presence of ternary membrane systems containing GM1 at the physiological concentration. SP is mostly unstructured in water, but appears as extended 3_{10} helical or turn III in isotropic bicelles, more pronounced in the presence of GM1. NMR results suggest that, in the GM1 containing bicelles, the peptide is more inserted into the membrane with its C-terminus, while N-terminus lies close to the membrane–water interface. The NMR-derived conformation of SP in GM1 bicelles is docked on homology modeled NK_1R and resulting interactions satisfy reported mutagenesis, fluorescence, photo-affinity labeling and modeling data. The results highlight efficacy of GM1 in membrane in providing structure in an otherwise flexible neurotransmitter Substance P; thus providing indication that it may be useful also for other neurotransmitter peptides/proteins associated with membrane.

© 2010 Elsevier B.V. All rights reserved.

1. Introduction

Structure evaluation of functional peptides is a promising field for drug development. Substance P (SP), the 11 amino acid neurotransmitter in central and peripheral nervous system is known to participate in a number of clinical syndromes like inflammatory bowel disease, inflammatory joint disease, interstitial cystitis, sickle cell disease, fibremylgia and diseases with chronic neuropathic and inflammatory pain in general [1,2]. Biological functionality of SP is mediated by its interaction with specific Neurokinin-1 receptor, which is a member of GPCR family. NK_1R and several hundreds of human GPCRs (s) are activated by extracellular protein or peptide ligands and peptide/protein-activated GPCRs represent a large, potential yet still underdeveloped source of new pharmaceutical targets for treating human diseases or medical conditions [3]. More than 120 GPCRs are inspected for which there are known peptide/protein ligands and statistics indicates that there is a common pattern or shape of the ligand peptide that is recognized by the receptor [4]. Frequently, turns or multiple turns (multiple α-turn as helix and β-turn as 3_{10} helix) are the motifs approved as common recognition scaffold.

In the classic model of GPCR signaling, receptors diffuse randomly in the lipid bilayer [5] and get activated by their corresponding neurotransmitters [6]. However, little is known about the events that mediate the membrane diffusion and activation of the receptor. It has been proposed that this receptor activated signaling cascade occurs through a clustering of components in a specific region of membrane where alteration of membrane homogeneity is necessary [7]. These heterogeneous regions are often rich in cholesterol and sphingomyelin with special enrichment in gangliosides [8,9] and are found to be functional in various neurological and psychiatric diseases through neurotransmitter signaling [6]. Yet, the role of gangliosides in neurotransmitter signaling remains elusive.

In fact, gangliosides at the neuronal membrane domains in dorsal root ganglia neurons (DRG) [10,11], cerebral cortex [12] and hippocampus [13] fix the possibility of regulating and organizing neurotransmitter signaling through GPCRs [6]. About 200 gangliosides are known today [14] which play important role in pathogenic mechanisms of many

Abbreviation: SP, Substance P; NK_1R, Neurokinin-1 receptor; GPCR, G-protein coupled receptor; GM1, Ganglioside Monosialo 1; DMPC, Dimyristoyl-sn-glycero-3-phosphorylcholine; CHAPS, 3-[(3-Cholamidopropyl) dimethylammonio]-1-propanesulfonate; GT1, Ganglioside Trisialo 1; GD1, Ganglioside Disialo 1; DOPC, Dioleoyl-phosphatidylcholine; DOPG, Dioleoyl-phosphatidylglycerol; POPC, Palmitoyloleoyl phosphatidylcholine; POPG, Palmitoyloleoyl phosphatidylglycerol; DHPC, Dihexanoyl-sn-glycero-3-phosphocholine; DPC, Dodecyl-phosphocholine; SDS, Sodium dodecyl-sulfate; NMR, Nuclear magnetic resonance; TOCSY, Total Correlation Spectroscopy; ROESY, Rotating-frame Overhauser Effect Spectroscopy; DQF-COSY, Double Quantum Filtered-Correlation Spectroscopy; ROE, Rotating-frame NOE; DOSY, Diffusion Ordered Spectroscopy; ADT, AutoDockTools

* Corresponding author. Tel.: +91 033 2351 8386; fax: +91 033 2351 9755.
E-mail addresses: chaitalicu@yahoo.com, cmchem@caluniv.ac.in (C. Mukhopadhyay).

0005-2736/$ – see front matter © 2010 Elsevier B.V. All rights reserved.
doi:10.1016/j.bbamem.2010.09.023

immune-mediated neurological disorders such as Guillain–Barre syndrome [15], Alzheimer's disease [16], Parkinson's disease [17] and Multiple System Atrophy (MSA) [18] among which notably ganglioside GM1 (Ganglioside Monosialo 1) is recognized for its functionality and specificity. GM1 serves as a receptor for Simian Virus 40 (SV40) [17], cholera toxin and shiga toxin [19] as well as acts as seed for formation of senile plaques in Alzheimer's disease [20] and internalizes monomeric α-synuclein into microglia, the key step in the pathogenesis of Parkinson's disease [17]. GM1 plays a broad spectrum of neurotrophic effects in vivo and in vitro. Treatment with GM1 partially restores the reduced pain perception in aged animals that claims localization of Substance P at the active site of GM1 function [21]. Contradictory reports declare that, GM1 has been discovered not to restore the reduced content of Substance P in spinal cord after peripheral-nerve injury and Substance P does not appear to be in active site of GM1 action [22]. Substance P is also found to bind preferentially to the negatively charged ganglioside monolayers showing the best interactions with complex gangliosides GT1>GD1>GM1 [23].

Structural studies of SP have been performed previously using membrane mimics like micelles, bicelles and vesicles. Darkes and Bradshaw using neutron diffraction method (for a DOPC:DOPG 50:50 bilayer) first showed that two population exists for tachykinin peptides like Substance P, one close to the water–membrane interface and other some 13 Å deeper [24]. Seelig and Macdonald observed that Substance P does not insert into the zwitterionic lipid monolayers (POPC), but does insert into the monolayers of negatively charged phospholipid (POPG) at the headgroup region [25]. Thermodynamic partitioning of Substance P in isotropic bicelles (q = 0.5) (DMPC/DHPC) is compared with partitioning in dodecylphosphocholine (DPC) micelles [26] wherefrom it is implicated that curvature of the membrane regulates the peptide partitioning. Weaver et al. interpreted that SP contains Type I and III beta-turns at N-terminus and virtually no helix at all when bound to negatively charged liposomes. Contradictingly, Keire and Fletcher proposed that C-terminus of the peptide with QFFG as α-helical turn lies at the periphery of DPC and SDS micelles despite of the micellar headgroup [27]. The same observation was reported by Cowsik et al. [28]. Recent reports, too, suggest evidence of unique conformational family of SP characterized by well-defined helix-like conformation consisting of nonstandard turns in the C-terminal (QQFFGLM) domain [29]. However, neither the biologically active conformation of Substance P (that is recognized by NK_1R) nor the effect of heterogeneous membrane mimics on its conformation has been unequivocally established.

The conformations adopted by Substance P are mostly random in water, whereas, 3_{10} helical or turn III spanning mid region residues Q6–G9 in zwitterionic bicelles and spanning C-terminal residues F8–M11 in bicelles containing GM1. Evidence of strong protection against paramagnetic quenching, decrease in translational diffusion coefficient as well as the presence of lipid–peptide cross peaks in NMR spectra imply that SP fairly penetrates in the GM1 containing membrane and turns out to be more ordered. Docking results also show that best fit is obtained when the GM1-induced conformation of SP is fitted at the NK_1R binding site thus providing justification for using ternary membrane system containing GM1 to study the bioactive conformations of membrane-active peptides.

2. Material and methods

2.1. Materials

The peptide Substance P, protonated DMPC (1,2-Dimyristoyl-sn-glycero-3-phosphorylcholine), CHAPS (3-[(3-Cholamidopropyl) dimethylammonio]-1-propanesulfonate) and deuterium oxide were purchased from Sigma Aldrich Pvt. Ltd. and used without further purification. GM1 was isolated and purified from goat brain in laboratory following the published protocol [30].

2.2. Bicelle preparation

Small isotropic DMPC/CHAPS (1:4) and DMPC/CHAPS/GM1 (1:4:0.3) bicelles were prepared using the published procedure [31]. Briefly, 5.0165 mg DMPC was initially suspended in water and vortexed and centrifuged for several times until homogenous slurry was formed, to which an aliquot of CHAPS from a 500 mM stock solution (in water of pH 5.5) was added to achieve q = 0.25 with a total lipid content in solution being 92.5 mM, where q is the concentration ratio of DMPC to CHAPS. The solution was then vortexed until a clear liquid was obtained. No pelleted lipid was separated from the solution after the centrifugation step. To prepare the GM1 containing bicelles, GM1 and DMPC were weighed first to prepare a homogenous solution of 3.46 mg GM1 and 5.0165 mg DMPC and then CHAPS was added in appropriate amount to make the solution clear as described earlier. The pH of the solution was adjusted only by adding small volumes of 1 M HCl or 1 M NaOH. Deionized water was used in preparation of the samples to avoid any salt interference.

2.3. NMR and CD sample preparation

For the NMR experiments and CD measurements 3.7 mM peptide was dissolved in DMPC/CHAPS (1:4), and DMPC/CHAPS/GM1 (1:4:0.3) bicelles [pH 5.5 at 298 K] to maintain peptide:lipid 1:25 mol/mol. The experiments were performed with freshly prepared samples though the bicelle samples without peptide were stable over months and the peptide containing bicelles were stable over weeks, if kept at −20 °C.

2.4. CD spectroscopy

CD spectra were acquired on a Jasco J-720 spectropolarimeter using a 0.1 cm path length demountable silica quartz cell at temperature 25 °C. Records were averaged over 5 scans collected at a speed of 20 nm/min over the interval 190 to 250 nm with 0.1 nm step resolution. Background spectra of bicelles were used as control and subtracted from each peptide spectra. CD curves were smoothed to 25 points, and the respective intensities are expressed in mean residue molar ellipticity $[\Theta] = 100\,[\Theta]_{obs}/CnL$, where $[\Theta]_{obs}$ is the observed ellipticity in mdegs, L is the optical path length in centimeters (0.1 cm), C is the final concentration of the peptide in molar, and n is the number of amino acids.

2.5. Solution NMR spectroscopy

The proton NMR spectra were recorded on a Bruker DRX 500 MHz spectrometer equipped with 5-mm broadband inverse probe head operating at a proton frequency 500.13 MHz. 10% D_2O was added for field frequency stability purpose and each spectrum was referenced to the HDO peak at 4.741 ppm. Suppression of the water signal was typically done by gradient methods of suppression using WATERGATE. Assignments of ^1H resonances of the backbone and side chains were made using a series of two-dimensional NMR experiments TOCSY, ROESY, NOESY and DQF-COSY, collected in the phase sensitive mode. Typically, sixteen scans were taken per increment. The spectral width was 6 kHz in both direct (F2) and indirect (F1) dimensions, with 2048 complex data points in F2 and 512 complex data points in F1. The TOCSY pulse sequence included 80 ms MLEV-spin lock, and the ROESY and NOESY spectra were acquired with mixing time of 300 and 350 ms. All 1D ^1H NMR spectra were processed using NMRPIPE software (spin.niddk.nih.gov/NMRPipe/). Two-dimensional NMR spectra were processed using XWINNMR version 3.75 (Bruker, Germany) and analyzed using SPARKY version 3.112 [32].

2.6. Spin label experiments

To further investigate the relative position of peptide in bicelles, paramagnetic quenching technique was used with Mn^{+2} as the

paramagnetic agent [33,34]. ^{1}H chemical shift spectra and TOCSY spectra of SP in bicelles (pH 5.5 at 298 K) were obtained after addition of 0.4 mM and 0.8 mM $MnCl_2$; and compared to the spectra of SP/PC bicelles and SP/GM1-PC bicelles before addition of $MnCl_2$. Experimental conditions and machine specifications were the same as described.

2.7. Translational diffusion experiments

DOSY experiments were carried out using a 500 MHz Bruker DRX spectrometer with a quad (^{1}H, ^{13}C, ^{19}F, ^{31}P) probe and z-gradient. Experimental conditions were the same as described earlier. The gradient coil constant was found to be 50 G/cm at 100% gradient strength by carrying out the BPLED pulse sequence with water suppression using pre-saturation. The diffusion time Δ was 150 ms and the gradient duration δ was 5 ms. The gradient strength was increased from 2 to 95% of Gmax in 32 scans. The DOSY spectra were constructed in the DOSY Toolbox (v 0.53) using fitting to a modified Stejskal–Tanner equation parameterized to take into account the effects of the pulse-field gradient non-uniformity [35]. Diffusion coefficient (DS) was calculated by fitting the curve of signal intensity versus variable gradient strength via use of MCR (Matlab Component Runtime). Exclude region command was used to correct the global noise and inconsistencies in the spectra affecting a particular signal intensity. Gaussian line shape with a single exponential fit was applied to each chemical shift of interest to optimize the resolution of signals.

The individual diffusion coefficients were calculated from the DOSY spectra using the selective acyl chain methylene and terminal methyl chemical shifts for DMPC and CHAPS, and, using aliphatic Leu-$H_{\delta1}/H_{\delta2}$ chemical shifts (about 0.89 ppm) for the peptide. The average bicellar diffusion coefficient was obtained by selecting specifically the non overlapping [36] aliphatic acyl chain methylene of DMPC (at 1.22 ppm) plus terminal methyl region protons of CHAPS (position 21 at 0.95 ppm, position 19 at 0.8 ppm, and position 18 at 0.6 ppm Fig. S13). The measured diffusion coefficient (D_{obs}) is given by the equation [37].

$$D_{obs} = \chi_{bound}.D_{bound} + \chi_{free}.D_{free}$$

or

$$D_{obs} = \chi_{bound}.D_{bound} + (1-\chi_{bound}).D_{free}$$

where χ_{free} and χ_{bound} are the mol fractions of free and bound peptide, respectively. D_{free} is obtained by measuring the diffusion coefficient of peptide in water, whereas, D_{bound} corresponds to the diffusion coefficient of the bicelles. However, in a bicelle environment, the diffusion of the free peptide is slowed down by the presence of bicelles themselves. Therefore, it is necessary to correct D_{free} by introducing an obstruction factor such as

$$D_{free}^{\phi} = D_{free}\langle A\rangle$$

where ϕ is the volume fraction of the obstructing particles, and $\langle A\rangle$ is a correction factor for spherical objects. This factor has been calculated as $\langle A\rangle = 0.95$ by Gaemers and Bax [38] for a 10% w/w bicelle solution at 20 °C assuming spherical shape of bicelles. Our bicelles, being proved to be spherical objects, account the perfect applicability of $\langle A\rangle$ [37].

2.8. Structure calculations

Sequence specific resonance assignments were done through the ^{1}H–^{1}H TOCSY cross peaks. ^{1}H–^{1}H ROESY cross peaks at 300 ms were assigned and integrated and the volumes were converted to distance restraints. When symmetric pairs of cross peaks were present, the larger peak volume was used and converted to the distance restraint. Cross peaks were categorized as strong, medium, weak and very weak based on their intensities. The interproton distances (r) were derived from the ROE intensities (S) with the known relationship $r = c(S)^{-6}$, where c is a coefficient determined on the basis of ROE corresponding to a known distance. The upper distance limits were normalized against the known distance of 3.05 Å for the $Phe_{HN\text{-}H\alpha}$ ROE for the non-aromatic proton ROEs and the 2.48 Å for the $Phe_{H\delta\text{-}H\varepsilon}$ for the aromatic proton ROEs [39]. The conservative upper distances were fixed respectively as 3.5, 4.0, 4.5 and 6.0 Å with a lower distance limit of 1.8 Å. Here, corrections of 0.5 Å were applied to the upper bound distances derived from ROEs to account for the spin diffusion effects. The dihedral angles (φ) were calculated from the $^{3}J_{HN\text{-}H\alpha}$ coupling constants measured from the DQF-COSY spectra using the Karplus relation $ACos^{2}\varphi + BCos\varphi + C = {}^{3}J_{HN\text{-}H\alpha}$, where $A = 6.98$, $B = -1.38$ and $C = 1.72$ with −60 degree phase difference in the dihedral φ. The values thus obtained were used as dihedral restraints. An error of 6° was accounted for ambiguity in selecting the centers of DQF-COSY cross peak contours. Structural calculations were performed using the XPLOR-NIH program [40]. 150 initial structures were generated from a random extended structure. The highest temperature that was achieved during the SA (simulated annealing) protocol was 3000 K, and the final lowest temperature that was achieved, was 12.5 K. A repel constant of 1.2 was used. The top seventy-five structures from the SA were further refined using the refinement protocol (refine.py) of XPLOR-NIH keeping the distance and dihedral restraints on. Several rounds of structure calculations were carried out, and depending on the NOE violations, the distance constraints were adjusted in each step. From the 75 structures, 40 best structures were finally selected on the basis of criteria of satisfactory covalent geometry, low distance constraint violations and favorable energy values. Final 3D structural figures were generated using VMD-XPLOR software package version 1.5 Linux 2.4_i686 running on Linux [41] and Pymol v0.99 running on Windows XP [42]. PSVS 3.1 server (psvs-1_3.nesg.org/) that includes PROCHECK NMR was used to evaluate the quality of the structures. VADAR server [43] was used to calculate the backbone and side chain hydrogen bonds.

2.9. Docking studies

The NK_1R was homology modeled using the M4T server [44] (multiple alignment models are 1hzxA, 2vt4B and 2hpyB and the region covered — residues 24–332). The NK_1R sequence used here consists of 364 residues starting from the N-terminus. Secondary structure of the EC2 loop as described in previous reports was incorporated in the receptor model [45–47]. Lowest energy structures of Substance P from the maximum populated ensembles in water and two bicelles were selected as ligands and were pre-optimized using the Autodock parameters like atom types, torsion modes and partial charges. Each peptide conformer was docked into the minimized receptor structure using Autodock4 software package from the Scripps Research Institute (http://autodock.scripps.edu).

An initial grid refinement according to the previously reported close contacts (Phe8/Met181, Gln4/Met174, Lys3/Met174 and Lys3/Glu21) between ligand SP and receptor NK_1R [48] was performed to ensure convergence of the computed expected values of the binding energy. The size of the grids and the grid spacing initially used as input were 50 × 50 × 50 Å and 0.375 Å. For the docking protocol, Lamarkian Genetic Algorithm (LGA) [49] was probed in order to find the most favorable interactions. For all dockings, the number of runs was set as 100. The number of energy evaluation was set to 25,000,000 while the population was set to 150. The 100 independent docking poses were clustered using ADT, and the lowest energy-docking pose from the cluster was recorded. The protein was taken as rigid and the side chains of the peptide were kept flexible during the docking. The best posing was selected depending on the highest binding energy criterion. Modeling of the figures showing the interactions at the binding site as well as hydrogen bonds from ligand to receptor residues was done using ADT.

2.10. Accession codes

Resonance assignments, distance and dihedral constraints, and ensemble of 40 NMR structures for Substance P in water, DMPC/CHAPS (1:4) and DMPC/CHAPS/GM1 (1:4:0.3) bicelles have been deposited to BMRB and SMSDep Bank under IDs 20115, 20116 and 20117 respectively. Five best docked SP-NK_1R complexes (using Autodock4) according to the magnitudes of binding energy using the NMR structures in water, DMPC/CHAPS (1:4) and DMPC/CHAPS/GM1 (1:4:0.3) bicelles as input have been deposited to RCSB Bank under IDs 2ks9, 2ksa, and 2ksb respectively.

3. Results

3.1. CD experiments

CD spectrum of Substance P (Fig. 1) in water shows a negative band around 202 nm with no positive band at all. This indicates that the peptide is mostly unstructured in water with a weak propensity to be in turn conformation. The peptide however is quite structured in the presence of bicelles. In both the bicelles, besides the main negative band at around ~202 nm, a small trough appears near 208 nm with increased ellipticity in the presence of GM1 suggesting the formation of transient helices that may persist with continuous exchange between turn and helical conformation. Minimum around 203 to 208 nm indicates overlapping helical and random coil $\pi\pi^*$ transition at 208 nm and 200 nm respectively. The similarity in the CD curves of the SP/PC bicelle and SP/GM1 bicelle indicates that the structured region of the peptide arranges itself almost in a similar manner in the two membrane mimetic environments. However, only the spectrum between 200 and 250 nm is shown as it was difficult to measure the spectrum for the bicelles below 200 nm due to scattering effect.

3.2. Chemical shift assignment and analysis

The chemical shifts of all protons of Substance P in water and bicellar environments are enlisted in Table S1 and the shifts in peak positions are depicted again in Fig. S2 (^1H–^1H TOCSY). The absence of a single set of proton chemical shifts for many protons indicates that a unique stable conformation is not possible for Substance P in either water or in bicelles. Broadening as well as signal attenuation of the α_H and aromatic proton peaks in Fig. 2C compared to Fig. 2A and B suggest that the peptide is not well exposed to the water phase but is partially located in or towards the GM1 containing membrane [50]. Fig. 3A and C show that

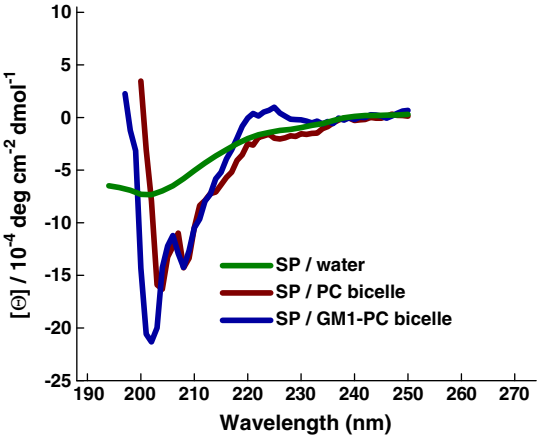

Fig. 1. Far-UV CD spectra of Substance P (3.7 mM) in water, DMPC:CHAPS (1:4) bicelles and DMPC:CHAPS:GM1 (1:4:0.3) bicelles at pH 5.5 and 298 K (peptide:lipid 1:25 mol/mol). Negative bands in the region 200–210 nm indicate ordered peptide structures. Individual plots are labeled in figure.

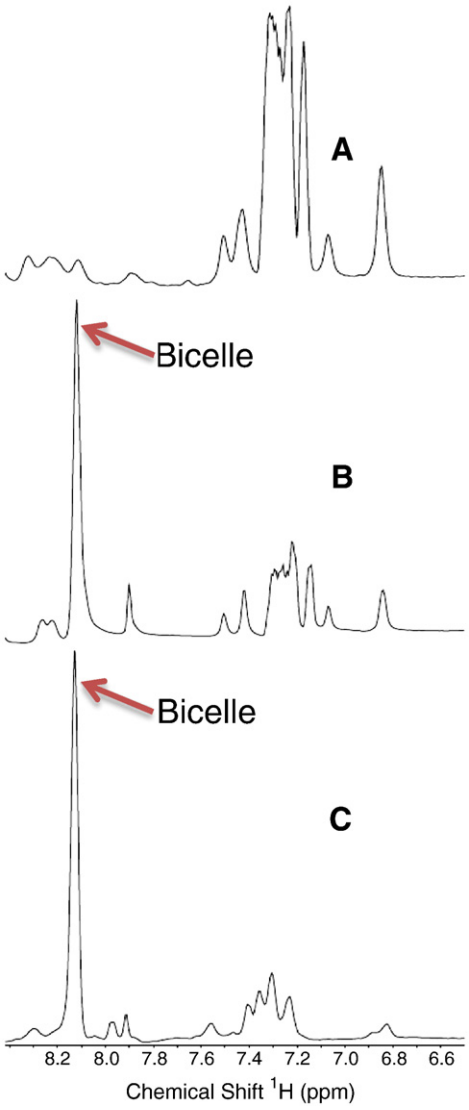

Fig. 2. ^1H NMR of Substance P (3.7 mM) in water (A), DMPC:CHAPS (1:4) bicelles (B) and DMPC:CHAPS:GM1 bicelles (C) at pH 5.5 and 298 K (peptide:lipid 1:25 mol/mol). The spectral region indicates the fingerprint aromatic and amide region (6.5–8.5 ppm). Broadening and signal attenuation of peaks are shown in (A)→(C). Peak due to the bicellar proton indicated with an arrow.

for residues 4–11, the difference in the chemical shift is consistently negative suggesting that this stretch of the peptide is basically helical or structured. A semi-quantitative estimation of the percentage of helical content of Substance P while going from water to either of the bicelles was obtained using the standard protocol by Wishart and coworkers, where the upfield shifts of the α_H protons [51] in the particular region assumed to be helical were averaged, and the averaged upfield shift was divided by 0.35 (0.35 ppm is assumed to correspond to 100% α-helix) [52]. The helical content of residues 4–11 for SP thus calculated was 17% in water, 22% in DMPC/CHAPS bicelle, and 36% in DMPC/CHAPS/GM1 bicelle. This α-helical character is significantly higher than that found in SP/DPC (10%) and SP/SDS (12%) [27]. The difference in the chemical shifts when compared to water depicts that, there is a strong propensity for the C-terminal amino acids to be involved in interaction with bicelles while the N-terminus remains flexible. Strong differences of α_H for Q5, Q6 and M11 in DMPC/CHAPS/GM1 bicelles when compared to the DMPC/CHAPS bicelle imply that these particular residues have a different conformation in the GM1 containing bicelles.

The NH proton chemical shift differences as shown in Fig. 3B and D provide general information about the hydrophobic/hydrophillic

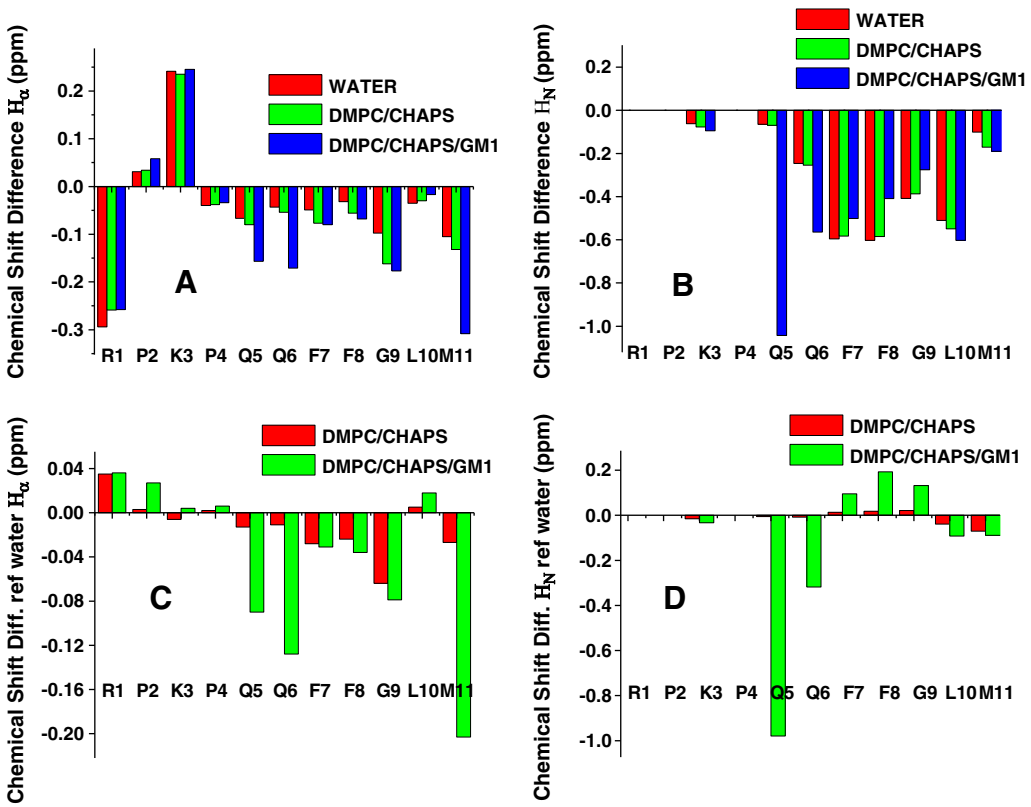

Fig. 3. Comparative alpha proton (A) and amide proton (B) chemical shift difference for Substance P (3.7 mM) in water, DMPC:CHAPS (1:4) and DMPC:CHAPS:GM1 (1:4:0.3) bicelles at pH 5.5 and 298 K (peptide:lipid 1:25 mol/mol). The chemical shift differences are calculated as Δ (observed proton chemical shifts) − (random coil chemical shifts) for each residue. Comparative differences in proton chemical shifts from water to DMPC:CHAPS and DMPC:CHAPS:GM1 bicelles are shown in (C) for alpha protons and (D) for amide protons. Colours of the bars are labeled in figure.

environment and hydrogen bonding network surrounding the corresponding protons. The amide NH secondary shifts for residues K3, Q5, Q6, F7, F8, G9, L10 and M11 show upfield values in water and bicelles with signal dispersion that indicate transient helical structure [53] in this region. However, significant shifts are observed for residues F7–L10 in all mediums that infer that these residues are at best involved in hydrogen bonding. Here, the small difference in resonance is thought to be due to the hydrogen bonding of backbone amide HN with –OH of water and large difference in resonance position is taken to be due to the hydrogen bonding of backbone amide HN with –O=C of peptide backbone or –O=C of neighbor lipid [54,55]. Surprisingly, in the GM1 containing bicelles, Q5 and Q6 (Fig. 3B) show noticeable hydrogen bonding propensity. The resonances of hydrophilic residues generally shift upfield relative to those of hydrophobic residues, which is a common signature of helical structure [53].

3.3. Paramagnetic quenching analysis

As the first approximation of the peptide positioning in bicelles, we have obtained the 1D ^{1}H chemical shift spectra of SP in both bicelles with varying concentrations of paramagnetic quencher $MnCl_2$ [33,34]. It is a known fact that, manganese ions affect the relaxation rate of the nuclei that are accessible to solvent and thus reduce the observed signal intensity. Since manganese ions cannot penetrate the hydrophobic interior of the bicelle, the change in the signal intensity can reflect the exposure of a particular nuclei; therefore facilitating the identification of residues closer to the aqueous phase. The 1D ^{1}H chemical shift spectra for finger print region of SP in DMPC:CHAPS and DMPC:CHAPS:GM1 bicelles are given in Fig. 4. Considerable decrease in signal intensities and broadening of spectral peaks were observed for SP/PC bicelles even at low $MnCl_2$ concentration (0.4 mM) in contrast to SP/GM1-PC bicelles. This suggests that the peptide is more exposed to the water phase in the absence of GM1. On the other hand, only partial reduction in signal intensities and broadening of spectral peaks are observed for SP/GM1-PC bicelles at 0.8 mM $MnCl_2$, which suggests that the peptide is more inserted in the bicelle hydrophobic interior in the presence of GM1.

The 2D ^{1}H–^{1}H TOCSY spectra (Fig. 5) of the peptide in both bicelles after addition of 0.8 mM $MnCl_2$ show a general broadening at the N-terminus of SP in PC bicelles (Fig. 5A and B); while the broadening is somewhat resisted in GM1 containing bicelles (Fig. 5C and D). Unaffected contours of Lys^3 in the presence of GM1 imply probable location of the residue away from the aqueous phase. These results are consistent with chemical shift deviations observed in Fig. 3.

3.4. Analysis of diffusion measurements

Translation diffusion measurements are summarized in Table 1, and the DOSY spectra are depicted in Figs. S3–S7. Diffusions of individual components are in agreement with the data previously been found [56–58] although under different experimental conditions. The diffusion of Substance P in aqueous solution is 28.3×10^{-11} m^2/s [59], which decreases in the different bicellar solutions, indicating that SP interacts with both the bicelles [56,57]. The diffusion coefficient is relatively lower for the bicelles containing GM1, which signifies the peptide motion being more constrained due to stronger interaction with bicelles in the presence of GM1. The results show that, 71% of the peptide is bound to GM1-PC bicelles, whereas 56% of the peptide is bound to PC bicelles. DMPC lipids are found to diffuse slower than CHAPS probably due to their size and the location of DMPC being at the bicellar disc region [56] compared to the location of CHAPS at the rim [57,58]. The

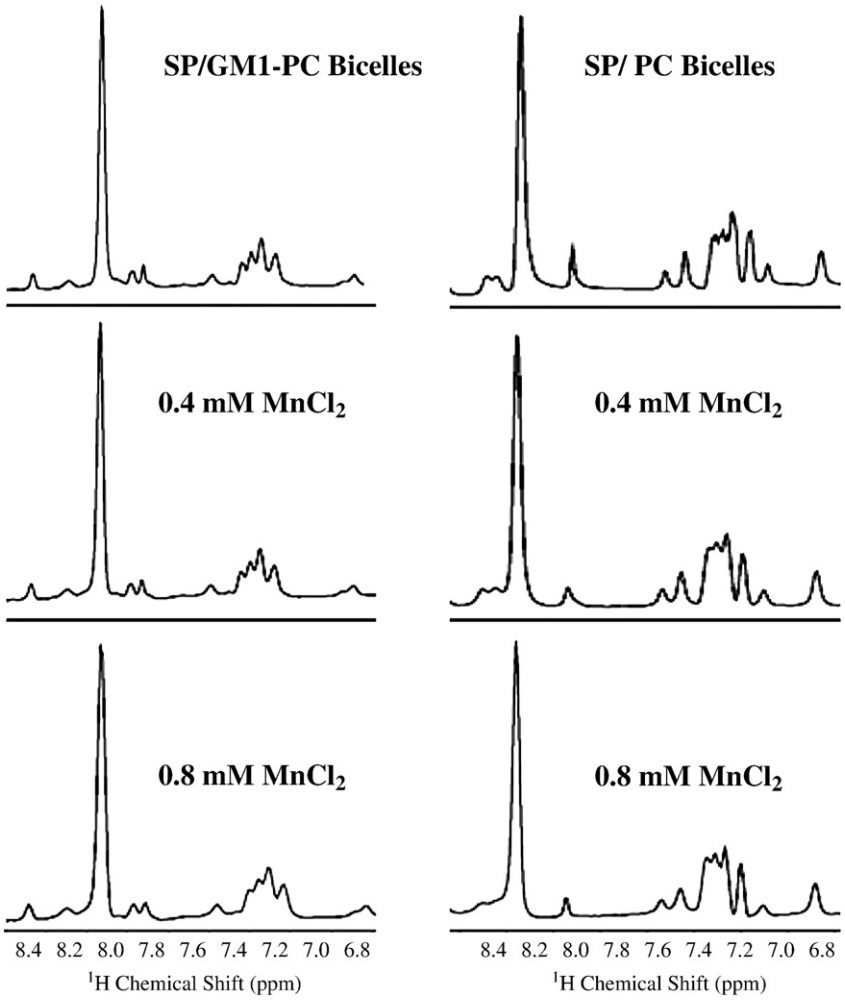

Fig. 4. The aromatic and amide proton chemical shift region of ^{1}H NMR spectra of Substance P (3.7 mM) in DMPC:CHAPS (1:4) and DMPC:CHAPS:GM1 (1:4:0.3) bicelles at pH 5.5 and 298 K (peptide:lipid 1:25 mol/mol) with (0.4 mM and 0.8 mM) and without $MnCl_2$. The comparison of spectra in the figure suggests that peptide peaks are broadened more efficiently in PC bicelles.

diffusion coefficient of DMPC decreases on addition of peptide in both the bicelles that suggests that peptide prefers to reside at the region of long-chain phospholipids [56,57]. Again, the presence of GM1 in bicelle reduces the diffusion coefficient of DMPC but not of CHAPS (11×10^{-11} m^2/s) implying the presence of GM1 amid the bicellar disc region.

3.5. NMR studies in water and bicelles — assignments and constraints

ROESY experiments (τ_{mix} 300 ms) were done at 1:13 and 1:25 peptide:lipid (mol/mol) ratio, and the ratio 1:25 was selected for distance calculation from cross peaks due to adequate number of cross peaks in 1:25 peptide:lipid. In the three solvent systems studied, the ROESY spectra (Figs. S8–S9) showed a fairly large number of short and medium range ROEs restricted mainly in the C-terminal region signifying partial conformational stabilization of this peptide segment. Noticeably, ROEs typical of α-helices were observed in none of the environments. By contrast, characteristic cross peaks of turn or 3_{10} helix were observed in bicelles over residues 4–11, that are d_{NN} (i,i + 1), d_{NN} (i,i + 2), $d_{\alpha N}$ (i,i + 1), $d_{\alpha N}$ (i,i + 2), $d_{\alpha N}$ (i,i + 3), and $d_{\alpha\beta}$ (i,i + 3) [60] (Fig. 6). Connective ROEs important to characterize the secondary structure of Substance P in different solvent medium are summarized in Fig. 6.

Simultaneous observation of various types of ROEs suggests some degree of conformational averaging occurring around a helical core. Possibility of β-turn and 3_{10} helix must be considered for the region near C-terminus as seen by the presence of $d_{\alpha N}$ (i,i + 2) at residues 7–9 in PC bicelles and at residues 4–6 and 9–11 in the GM1 containing bicelles [61]. Moreover, $d_{\alpha N}$ (i,i + 3) at residues 4–7 and 7–10 in DMPC/CHAPS bicelles and $d_{\alpha\beta}$ (i,i + 3) at residues 3–6 and 5–8 in DMPC:CHAPS:GM1 bicelles (Fig. 6) may provide additional hydrogen bond interactions that stabilize short length helical structure in small linear tachykinin peptides like Substance P [62].

It is also possible to acquire information about the peptide secondary structure from the backbone phi (φ) angles along the peptide chain by measuring $^3J_{N\alpha}$ (Hz) coupling constants. The coupling constants are enlisted as the top panel in Fig. 6. Helical structures appear with coupling constants 4–5 Hz, whereas extended structures have coupling constants in the range 8–9 Hz [63]. All coupling constants for Substance P in water and the bicelles were found to be ~8 Hz that suggest that the structures are not typically helical. Instead, large $^3J_{N\alpha}$ coupling constants indicate that most of the residues are involved in turn conformations [63,64]. The magnitudes of the coupling constants are comparatively lower for SP in the GM1 containing bicelles.

3.6. Solution structure of Substance P in water and bicelles

Forty refined structures obtained in each medium that had passed the acceptance criteria were put in ensembles named A, B and C (for water, PC bicelle and GM1 bicelle respectively) and were selected for further analysis. The statistical summary of the peptide structures along with information regarding the backbone dihedrals and H-bonding interactions in different medium are provided in Table S11. In water, the conformers are grouped in three ensembles (Fig. 7, panel A) where the

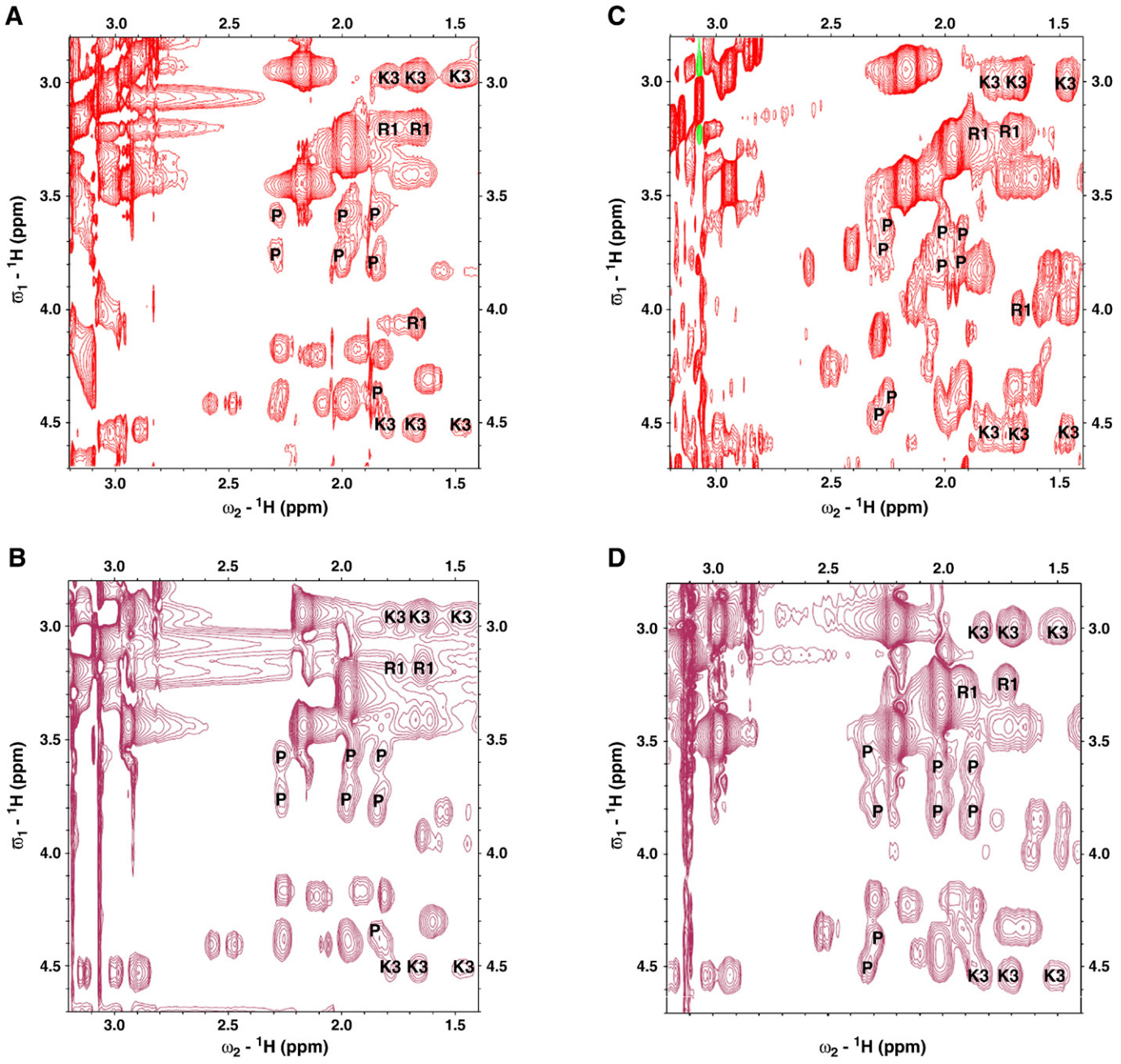

Fig. 5. Affected N-terminus in 2D ^{1}H–^{1}H TOCSY spectra of Substance P (3.7 mM) in DMPC:CHAPS (1:4) (A and B) and DMPC:CHAPS:GM1 (1:4:0.3) (C and D) bicelles at pH 5.5 and 298 K (peptide:lipid 1:25 mol/mol) without and with 0.8 mM $MnCl_2$ respectively. Amino acid signals suffering from the paramagnetic quenching are labeled in the figure.

Table 1
Measured translational diffusion coefficients of Substance P and bicellar components DMPC and CHAPS in solution using DOSY and calculated fraction (%) of peptide bound to bicelles (pH 5.5 and 298 K).

	$D_{obs} \pm 0.1$ ($\times 10^{11}$ m^2/s)				
Samples	SP	DMPC	CHAPS	Bicelle	% bound
SP/water	28.3[a]				
DMPC:CHAPS bicelle		9.38[b]	11.0[b]	9.56	
SP/DMPC:CHAPS bicelle	17.0	9.22	11.9	9.52	56
DMPC:CHAPS:GM1 bicelle		9.04[c]	10.9	9.25	
SP/DMPC:CHAPS:GM1 bicelle	14.4	8.81	11.2	9.16	71

[a] 25.3 ($\pm$0.5%) $\times 10^{11}$ m^2/s in water (Ref. [59]).
[b] In [DMPC]:[CHAPS] = 0.5, D_{DMPC} 5.8 $\times 10^{11}$ m^2/s and D_{CHAPS} 6.5 $\times 10^{11}$ m^2/s (Ref. [57]).
[c] In [DMPC + DMPG]:[DHPC] = 0.15, D_{DMPC} 9.4 $\times 10^{11}$ m^2/s (Ref. [58]).

populations comprise 67.5, 20 and 12.5% conformers respectively. Residues 6–9 are found to have turn III structure (36.4%) but the entire peptide is still a coiled coil as evaluated by DSSP [65]. This result is consistent with the results obtained in previous NMR and CD experiments where it was found that the free acid form of Substance P in water adopts an extended conformation at the N-terminus and a helical conformation at the C-terminal segment of the peptide though the helix content of SP in water is practically negligible [66–70]. Raman spectra of SP in water, too reported that SP forms an ensemble of conformers in water which is distinctly different from completely unfolded peptide conformation [71]. Backbone hydrogen bonds, as determined from VADAR, exist between Gln6 and Gly9, Gln6 and Leu10, and Phe7 and Leu10 with mean H-bond distance 2.55 Å (data not shown). The significance of H-bonding from NH-protons of Gly^9, Leu^{10}, and Met^{11} was also observed by Bundi and Wüthrich et al. [72]. No side chain

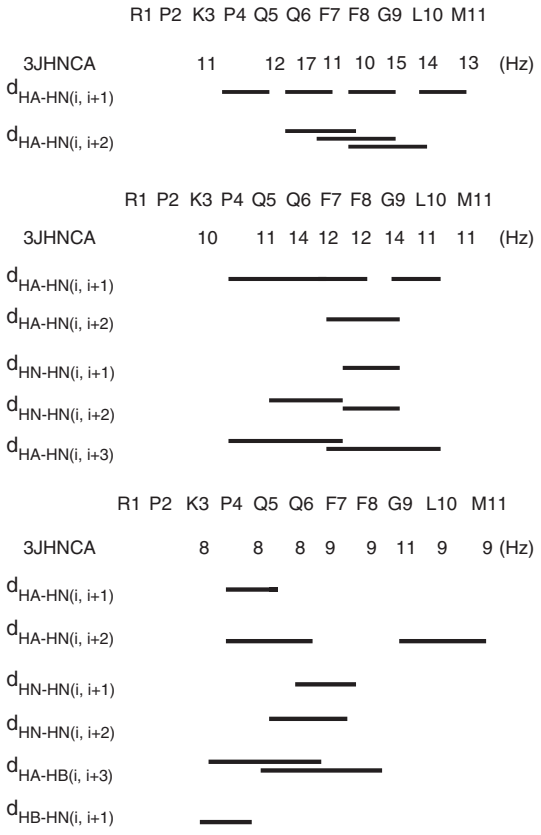

Fig. 6. Coupling constants and ROE connectivity plots for sequence of Substance P in water (top panel), DMPC:CHAPS bicelles (1:4) (middle panel) and DMPC:CHAPS:GM1 (1:4:0.3) (bottom panel) bicelles at pH 5.5 and 298 K (peptide:lipid 1:25 mol/mol) showing the ROE connectivity among residues.

hydrogen bonds were observed. According to the Ramachandran plot, 99.6% of total residues lie in the allowed region (Fig. S10). Most of the residues adopt an irregular orientation and no preference exists for distribution of polar and nonpolar residues in water.

Substance P structures in DMPC/CHAPS bicelles also ungroup as in three ensembles as shown in Fig. 7 (panel B), where the first sub-ensemble with population 82.5% reflects mostly the family. Residues K3–Q6 are found to form a turn III structure, which closely resembles the 3_{10} helix. Residues K3, P4, Q5, Q6, F7, F8 and G9 were found to be involved in backbone hydrogen bonding, as evaluated by VADAR (data not shown). Here C=O of Lys3, Pro4, Gln5 and Gln6 act as acceptors whereas HN of Gln5, Gln6, Phe7, Phe8 and Gly9 serve as the donors. The mean H-bond distance is 2.8 Å. Side chain hydrogen bonds appear between NE2 of Gln5, Gln6 and O=C of Lys3. The 3_{10} helix or turn III is depicted also from phi–psi magnitudes of the second and third residues of the turn. According to the Ramachandran plot, 100% of total residues lie in the allowed region (Fig. S10). Side chains of residues F7, F8 and L10 are found to lie on one side of the peptide backbone whereas polar R1, K3, Q5 and Q6 side chains are positioned towards the opposite direction. Distributional division of the hydrophobic and hydrophilic residues may help the arrangement in which the peptide orients itself towards the DMPC/CHAPS membrane.

Once again, the sub-ensemble presented in the first column of C appears as the representative of total SP conformers when studied in the environment of GM1 containing bicelles. Residues 8–11 (36%) are found to adopt turn III structure, which closely resembles the 3_{10} helix. R1, K3, Q5, Q6, F7, F8, G9, L10 and M11 are involved in backbone hydrogen bonding where Phe8 is the maximum contributing residue (data not shown). In this case, the acceptors are C=O of Arg1, Lys3, Gln5, Gln6, Phe7 and Phe8 and donors are HN of Lys3, Gln5, Gln6, Phe7, Phe8, Gly9 and Met11 respectively. The mean H-bond distance is 2.6 Å. Side chain hydrogen bonds appear between NE2 of Gln6 and O=C of Pro4. 100% of the residues lie in the favored region of Ramachandran plot (Fig. S10).

4. Discussion

Detergent micelles have long been used as membrane mimicking media in spectroscopic investigations, but lately two-component micelles and bicelles emerge as suitable experimental membrane models. However, peptide conformation and dynamics may be influenced by small size and shape of micelles where bicelles turned out to be superior [56]. The use of bicelles as membrane mimics in the present study can be justified from some recent reports that establish higher morphological and compositional similarity of bicelles to native bilayers. Donghan et al. recently reported that in small bicelles (DMPC/DHPC) a bilayer is formed which successfully solubilize the intact outer membrane protein OmpX from *Escherichia coli* [73]. In another report Kang et al. have shown that bicelles (DMPG/DHPC) can deliver a functional membrane protein KCNE3 to oocyte membrane that expresses human KCNQ1 channels [74]. In our laboratory we have successfully prepared ternary bicelles composed of DMPC, CHAPS and ganglioside GM1 and reported it to be useful in imparting specific conformation to opioid peptide like leucine enkephalin [31]. In a very recent report DMPC/CHAPS/GM1 ternary bicelle with $q = 0.5$ has been used as biologically relevant membrane environment for insertion depth and orientation of gangliosides relative to the membrane surface characterization [75]. In the report, the concentration of GM1 is only ~1 mol% of the entire bicelle whereas in our experiment GM1 is 5.66 mol% of total bicellar mass. Reasons behind the choice are: i) increase of surface charge due to sialic acid (anionic lipids 25–30 mol% of phospholipids are used in bicelles to make the bicelles anionic) [37,76] ii) 5–10 mol% GM1 is found to be present in ganglioside enriched domains (caveolae) of neuronal plasma membranes [77]; and, consequently iii) 5 mol% GM1 in membrane has been experimentally found to interact with functional proteins like Protein Kinase C (PKC), Wheat Germ Agglutinin (WGA), Cholera Toxin B subunit, Sphingolipid Activator Proteins (SAP-B) and Simian Virus 40 (SV40) [78–81]. CHAPS is used in this study as an alternate of cholesterol. Though CHAPS is a detergent and cholesterol is a lipid, both CHAPS and cholesterol are reported to increase the similar rigidity of membrane by increasing the order of acyl chains of phospholipids because of similarity in their molecular structure regarding the sterol region [82–84].

To verify that GM1 present in ternary bicelles is more potent to impact biologically relevant conformation to Substance P, we have recorded CD experiments with SP in the presence of CHAPS/GM1 mixed micelles with varying GM1 concentration (the details of the mixed micelle preparation, DLS experimental procedure and CD spectra are provided in Supporting Information S12). Though DPC/GM1 is the popularly known mixed micelle containing GM1 [85,86], we have chosen CHAPS instead of DPC (dodecyl phosphocholine) because CHAPS is an essential component of our ternary bicelles and it has the similar ability as DPC to protrude the ganglioside hydrophilic portion from the membrane plane to extracellular fluid which assists the GM1-selective bindings of foreign bio-molecules [87]. A monomodal distribution found in DLS (Fig. S12A) clarifies the presence of mixed micelles in experimental solutions when compared to CHAPS micelles only. It is apparent from the CD spectra (Fig. S12B) that even in the presence of 0.7 mM GM1, the ellipticity is only 43% of the SP/GM1 bicelles and the helical signature is absolutely absent.

While the CD spectra suggests an equilibrium between helical and turn conformations in both the bicelles (Fig. 1), the NMR studies predict a significant helicity from upfield chemical shift differences (Fig. 3), what can be termed as "nascent helix" [53]. 2D ^1H–^1H ROESY of Substance P (Figs. S8, S9) show patterns characteristic of turns and 3_{10} helices in both the bicelles whereas signature of pure α-helices, $d_{\alpha N}(i,i+4)$ is absent in all (Fig. 6). Ramachandran plot (Fig. S10) predicts that turn III or 3_{10} helix is the probable peptide conformation in the bicelles spanning residues

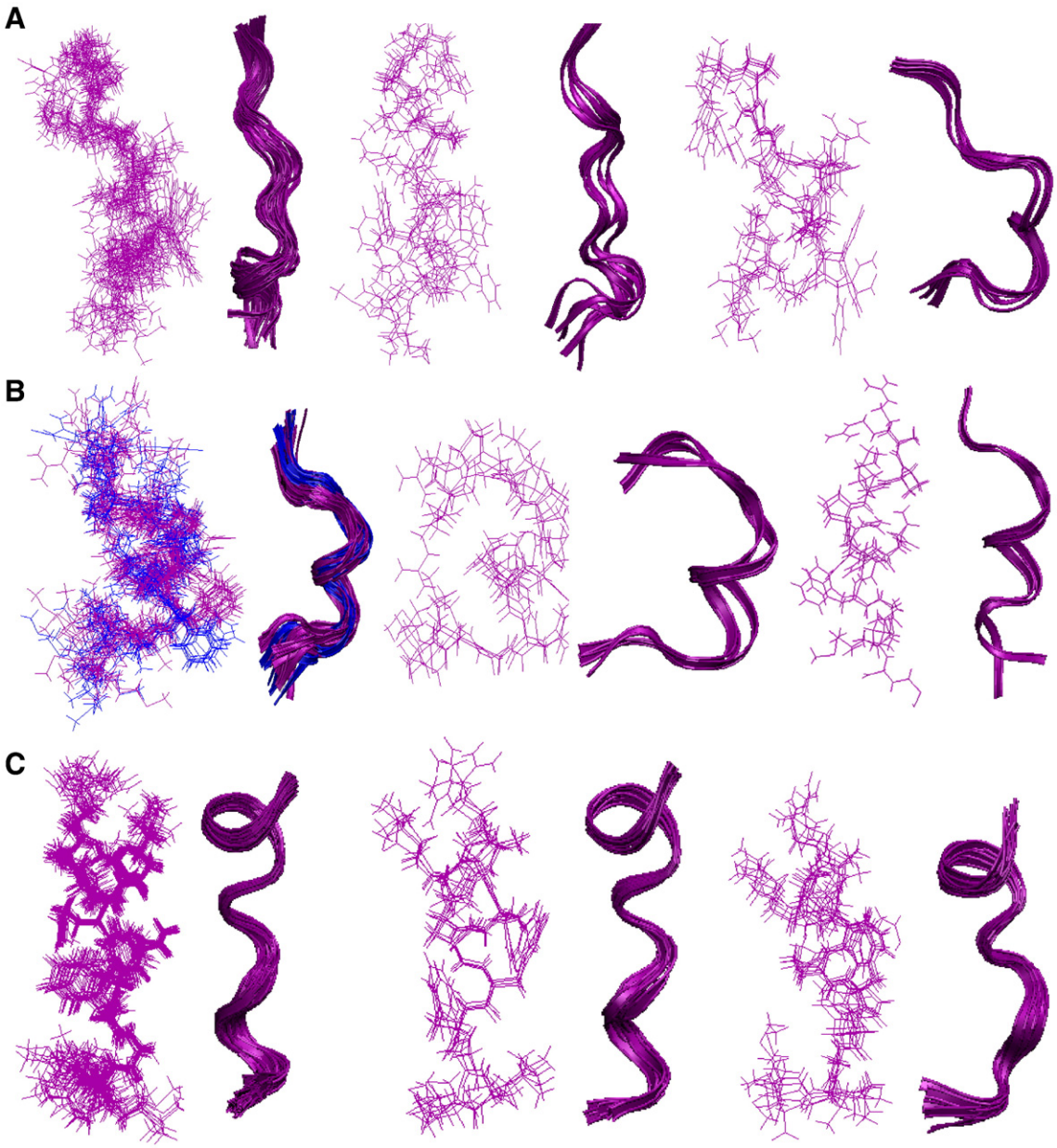

Fig. 7. Line and ribbon representations of ensembles of 40 structures of Substance P (3.7 mM) in water (A), DMPC:CHAPS bicelles (1:4) (B), and DMPC:CHAPS:GM1 (1:4:0.3) (C) bicelles at pH 5.5 and 298 K (peptide:lipid 1:25 mol/mol). Superimposition of sub-ensembles of 40 conformers was done using VMD-XPLOR. Conformations that differ in side chain orientations but have similar backbone are shown in blue.

3–6 in DMPC/CHAPS [26–28,88] and 8–11 in DMPC/CHAPS/GM1. In PC bicelles, the distance αH_i–αH_{i+3} is about ~6 Å, while in the GM1 containing bicelle, it is ~7 Å. Characteristic of a specific turn signature is αH_i–αH_{i+3}~7 Å. ROE connectivity (Fig. 6) as well as αH_i–αH_{i+3} distances suggests a turn structure in bicelles which is a good signature for suitability of membrane penetration and GPCR-recognition [4]. Recently in a paper by Mobashery et al., a similar conserved conformation is found for Penicillin-binding protein 5 (PBP 5) C-terminus (EGNFFGKIIDYIKLMFHHWFG) where the turn and bend motifs only rule the penetration in the membrane [89].

Intense diagonal peak of Lys^3 is observed in the GM1 containing bicelles (Fig. S9) that does not disappear when paramagnetic quencher Mn^{+2} is added (Fig. 5). Similar observations were also found from differences in chemical shifts (Fig. 3). The presence of strong backbone H-bonds between Lys^3 and Gln^5 in NMR conformers also suggests that, the lysine residue crosses just the interface to remain close to the bicelle interior and appear less hydrated [42]. Beside this, when compared between the broadening of all N-terminal amino acids in bicelles in general, moderate quenching of the signals at a relatively low concentration of $MnCl_2$ suggests that SP bound to PC bicelles is more exposed (Fig. 5).

In ROESY (Fig. S9), Gln6 side chain NH2 (trans) and Gln5 side chain NH2 (trans) protons [82] positions are merged in water and zwitterionic bicelles while they differ in chemical shifts in the bicelles containing GM1. Moreover, the Gln6 NH2 (cis) diagonal peak intensity decreases and the Gln6 NH2 cis–trans cross peak disappears in the bicelles containing GM1. Thus, the two glutamine residues behave in a different way in the presence of GM1 [90]. Also, Gln6 may be present in a restricted environment where the conformation is arrested with the side chain amine NH2 at the trans-position only.

In the ROESY spectra of SP in GM1 containing bicelles (Fig. 8), columns in the aromatic region (at 7.1 to 7.4 ppm) exhibit cross peaks

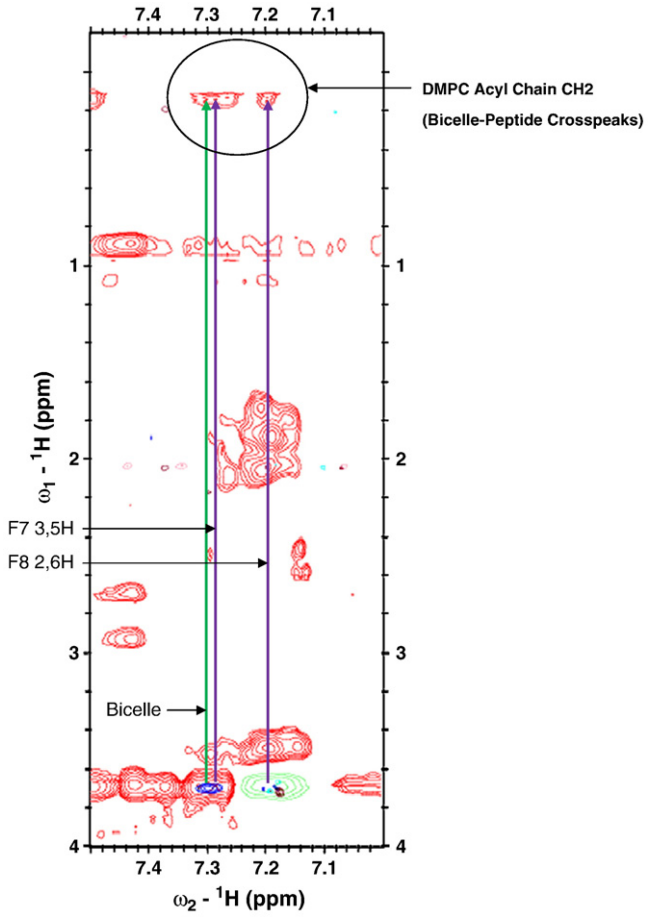

Fig. 8. 2D ^{1}H–^{1}H ROESY region showing the cross peaks of Substance P aromatic protons with lipid acyl chain –CH2– protons of DMPC in DMPC:CHAPS:GM1 bicelles (1:4:0.3) at pH 5.5 and 298 K (peptide:lipid 1:25 mol/mol). The control DMPC:CHAPS:GM1 bicelle contours are shown in blue. The violet lines indicate the strips of lipid–peptide cross peaks. The green line indicates a resonance of lipid from DMPC:CHAPS:GM1 bicelle close to the peptide resonance but with measurable chemical shift difference.

to lipid resonances that are absent in the zwitterionic bicelles. The most intense cross peaks at 1.23 ppm correspond to the methylene protons of the lipid acyl chains [91]. The peak at 7.28 ppm is for F7 3,5 H (H_{ε}) and at 7.19 ppm is for F8 2,6 H (H_{δ}). Cross peaks between protons at 7.28 ppm and 7.19 ppm to the proton at 1.23 ppm indicate that the aromatic group protons are close in space with the acyl chain protons of DMPC indicating that the phenylalanine residues penetrate into the hydrocarbon core of the membrane. The relative intensity of the cross peaks compared to diagonals (data not shown) implicates that Phe^{8} is more inserted in membrane than Phe^{7}. To verify whether the cross peaks arise due to the interaction of the lipid acyl chains to the aromatic residues, ROESY spectra were obtained without the peptide in each bicelles (shown as violet contour in Fig. 8). The spectrum peaks due to only bicellar lipids appear in the spectra but the lipid–peptide cross peaks disappear. The glycerol and choline protons of DMPC appear at same resonances in the presence and absence of the peptide (spectra not shown) that indicates that DMPC lipid headgroup is not altered noticeably when Substance P binds to the GM1 containing bicelles [92]. The probable location of SP in GM1 containing bicelles is corroborated well with the previous report by Seelig et al., where mutational studies on SP were performed (G9R) and weak penetration with low hydrophobic binding constants in the negatively charged membrane was found [93].

Table 2
SP/NK_1R docking results: environments, computed binding energies, inhibition constants, and proximal residues of NK_1R to SP.

Environments	Binding energy (kcal/mol)	Inhibition constant (μM), K_i	Proximal residues of NK_1R to SP
Water	−2.79	9020	Val4, Asp10, Thr17, Ser20 and Glu21
DMPC:CHAPS bicelles (1:4)	−4.17	871.13	Asp10, Ile15, Ser16, Ser20 and Thr19
DMPC:CHAPS:GM1 bicelles (1:4:0.3)	−4.26	754.14	Leu5, Pro13, Ile15, Ser16, Thr17, Ser20, Leu102 and Leu103

Translational diffusion coefficients indicate that the presence of GM1 hinders the bicelle diffusion due to constrained mobility of long-chain phospholipids. Gangliosides are large molecules with two hydrocarbon chains along with a large oligosaccharide headgroup and are located mostly in the upper leaflet of the cell membrane in proximity towards the extracellular space fluid. Though direct diffusion coefficient measurement for GM1 is impossible here, its impact is clearly shown. The peptide diffusion is slowed down in each bicelle; however, the presence of GM1 makes the peptide slower that means peptide interacts stronger with the membrane in the presence of GM1. The partition of the peptide is found to be 71% in DMPC:CHAPS:GM1 bicelles when compared to 56% in DMPC:CHAPS bicelles that deliberately support the idea of better penetration of SP in the hydrophobic region of the bicelles.

To gain insight into the NK_1R interaction mode, we have performed a docking where representative conformations from the highest populated ensembles were docked onto the homology modeled NK_1R (Table 2). For clarity, the SP NMR models in water, DMPC:CHAPS bicelles and DMPC:CHAPS:GM1 bicelles are termed as SPA, SPB, SPC and the docked complexes are termed as NKSPA, NKSPB and NKSPC (Fig. 9). From Table 2, it is reflected that the binding energy increases two fold when the peptide conformer is changed from NMR model of SP in water to either of the bicelles. The NMR conformation of SP in GM1 containing bicelles when docked on NK_1R shows the highest binding energy and lowest inhibition constant to NK_1R, which indicates that it fits best to the active site of NK_1R. The residues that are present in the binding site are depicted in Figs. 9, S14 and Table 2. Hydrogen bonds are formed only in NKSPC from Arg1 of SP to Pro13 of NK_1R, and Gln5 of SP to Ser20 of NK_1R (Fig. S14) (backbone rmsd after docking does not deviate from 0.01 Å). In NKSPC, Lys^{3} of SP is found in close proximity of Ser16 and Thr17 (N-terminus of NK_1R) [42]. Also the C-terminus residues Phe^{7}-Met^{11} were found to interact with the receptor first extracellular loop EC1 (Leu102 and Leu103) over TM3 [94]. The possibility of this type of binding mode is already inferred by Mierke et al. [48].

5. Conclusion

Experimental results combining the CD and NMR data suggest that SP adopts a conserved turn structure in isotropic bicelles with a preference to GM1 containing bicelles. The differences in the composition of the membranes come out to be responsible for the different binding affinity of the peptide to the membranes, and hence the diversity of the peptide structures. Previous studies from our lab show that GM1 containing bicelles can distinctly modulate the bioactive structure of opioid peptides like leucine enkephalin. This paper establishes that GM1 containing bicelles can yet serve as suitable native-like membrane environment and induce “receptor-binding” conformation to an otherwise flexible neurotransmitter Substance P. As the interaction between SP and its receptor NK_1R is specific in caveolae where GM1 is abundant, the conformation that emerges from our study may closely resemble the bioactive conformation of the peptide. Further study involving modification of bicelle composition with other gangliosides is in progress in our laboratory.

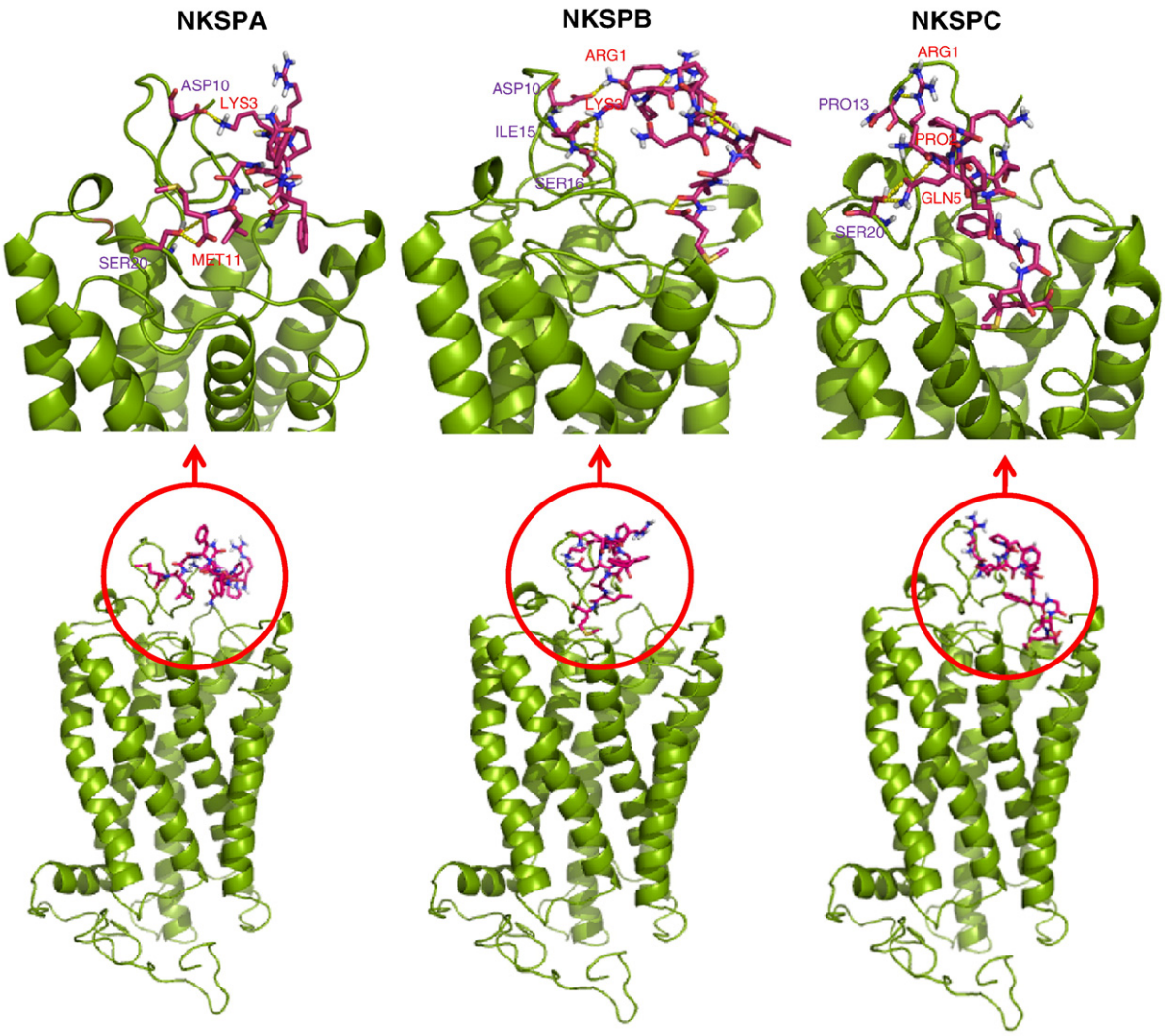

Fig. 9. Bound-state structure representation of Substance P to NK_1R after docking using Autodock. NK_1R is coloured green and displaying secondary structure (bottom panel). The figures in the upper panel originating from the docked complexes in bottom panel indicate docking sites of NKSPA, NKSPB, and NKSPC, where SP docked on homology modeled NK_1R where SPA, SPB and SPC indicate one of the abundant NMR conformers (Fig. 7) in water, DMPC:CHAPS bicelle and DMPC:CHAPS:GM1 bicelle respectively. The peptide SP is coloured according to atom representations and displaying ball and stick licorice model. Amino acid residues of ligand peptide are labeled in red whereas amino acid residues of receptor NK_1R are coloured violet. The sub-sections of this figure were prepared using ADT viewer and Pymol.

Acknowledgements

We thankfully acknowledge Central Facility of Saha Institute of Nuclear Physics, Kolkata for the CD measurements; Bose Institute and Indian Association for the Cultivation of Science, Kolkata for the NMR experiments. Central facility of Bose Institute, Kolkata is acknowledged for the DLS experiments. This work acknowledges financial support of CSIR grant CSIR-01 (2035)/06/EMR-II. A.G. is thankful for UGC fellowship under award no. UGC/320/Fellow/Univ.

Appendix A. Supplementary data

Supplementary data to this article can be found online at doi:10.1016/j.bbamem.2010.09.023.

References

[1] S. Harrison, P. Geppetti, Substance P, Int. J. Biochem. Cell Biol. 33 (2001) 555–576.
[2] T.J. Dougherty, M.J. Pucci, J.J. Bronson, D.B. Davison, J.F. Barrett, Antimicrobial resistance — why do we have it and what can we do about it? Expert Opin. Investig. Drugs 9 (2000) 1707–1709.
[3] P.D. William, M.C. Kathleen, G protein-coupled receptors as potential drug Targets for lymphangiogenesis and lymphatic vascular diseases, Arterioscler. Thromb. Vasc. Biol. 29 (2009) 650–656.
[4] J.D.A. Tyndall, B. Pfeiffer, G. Abbenante, D.P. Fairlie, Over one hundred peptide-activated G protein-coupled receptors recognize ligands with turn structure, Chem. Rev. 105 (2005) 793–826.
[5] S.J. Singer, G.L. Nicolson, The fluid mosaic model of the structure of cell membranes, Science 175 (1972) 720–731.
[6] J.A. Allen, R.A. Halverson-Tamboli, M.M. Rasenick, Lipid raft microdomains and neurotransmitter signalling, Nat. Rev. Neurosci. 8 (2007) 128–140.
[7] R.V. Rebois, T.E. Hebert, Protein complexes involved in heptahelical receptor-mediated signal transduction, Recept. Channels 9 (2003) 169–194.
[8] A.A. Wolf, M.G. Jobling, S. Wimer-Mackin, M. Ferguson-Maltzman, J.L. Madara, R.K. Holmes, W.L. Lencer, Ganglioside structure dictates signal transduction by cholera toxin and association with caveolae-like membrane domains in polarized epithelia, J. Cell Biol. 141 (1998) 917–927.
[9] P.H.H. Lopez, S. Ronald, Gangliosides in cell recognition and membrane protein regulation, Curr. Opin. Struct. Biol. 19 (2009) 549–557.
[10] Y. Sakumoto, H. Ueta, N. Yuki, K. Matsuno, Simultaneous immunohistochemical detection of gangliosides and neuronal markers in paraformaldehyde-fixed nervous tissues by acetone etching, Arch. Histol. Cytol. 72 (2009) 77–90.
[11] S.U. Kim, G. Moretto, V. Lee, R.K. Yu, Neuroimmunology of gangliosides in human neurons and glial cells in culture, J. Neurosci. Res. 15 (1986) 303–321.
[12] M. Siomara, S. Francieli, V. Luciene, M. Cristiane, B. Jaqueline, B. Adriane, T. Vera, W. Angela, Ovariectomy enhances acetylcholinesterase activity but does not alter ganglioside content in cerebral cortex of female adult rats, Metab. Brain Dis. 20 (2005) 35–44.

[13] J.-Q. She, M. Wang, D.-M. Zhu, L.-G.L. Sun, D.-Y. Ruan, Effect of ganglioside on synaptic plasticity of hippocampus in lead-exposed rats in vivo, Brain Res. 1060 (2005) 162–169.
[14] T. Ariga, M.P. McDonald, R.K. Yu, Thematic review series: sphingolipids. role of ganglioside metabolism in the pathogenesis of Alzheimer's disease — a review, J. Lipid Res. 49 (2008) 1157–1175.
[15] H.J. Willison, N. Yuki, Peripheral neuropathies and anti-glycolipid antibodies, Brain 125 (2002) 2591–2625.
[16] Y. Ohmi, O. Tajima, Y. Ohkawa, A. Mori, Y. Sugiura, K. Furukawa, K. Furukawa, Gangliosides play pivotal roles in the regulation of complement systems and in the maintenance of integrity in nerve tissues, Proc. Natl. Acad. Sci. 106 (2009) 22405–22410.
[17] J.-Y. Park, K.S. Kim, S.-B. Lee, J.-S. Ryu, K.C. Chung, Y.-K. Choo, I. Jou, J. Kim, S.M. Park, On the mechanism of internalization of α-synuclein into microglia: roles of ganglioside GM1 and lipid raft, J. Neurochem. 110 (2009) 400–411.
[18] V. Cullen, M. Lindfors, J. Ng, A. Paetau, E. Swinton, P. Kolodziej, H. Boston, P. Saftig, J. Woulfe, M.B. Feany, L. Myllykangas, M.G. Schlossmacher, J. Tyynela, Cathepsin D expression level affects alpha-synuclein processing, aggregation, and toxicity in vivo, Mol. Brain 2 (2009) 5.
[19] B. Tsai, J.M. Gilbert, T. Stehle, W. Lencer, T.L. Benjamin, Gangliosides are receptors for murine polyoma virus and SV40, EMBO J. 22 (2003) 4346–4355.
[20] M. Wakabayashi, K. Matsuzaki, Formation of amyloids by Aβ-(1–42) on NGF-differentiated PC12 cells: roles of gangliosides and cholesterol, J. Mol. Biol. 371 (2007) 924–933.
[21] C. Fromm, J.A. DeLeo, D.W. Coombs, R.W. Colburn, B.B. Twitchell, The ganglioside GM1 decreases autonomy but not Substance P depletion in a peripheral mononeuropathy rat model, Anesth. Analg. 77 (1993) 501–506.
[22] V.M. Goettl, A.E. Lindsey, N.H. Neff, M. Hadjiconstantinou, Gm1 ganglioside restores abnormal responses to acute thermal and mechanical stimuli in aged rats, Brain Res. 858 (2000) 380–385.
[23] M. Gonzalez, N. Lezcano, M.E. Celis, G.D. Fidelio, Interaction of alpha-MSH and substance P with interfaces containing gangliosides, Peptides 17 (1996) 269–274.
[24] M.J.M. Darkes, S.M.A. Davies, J.P. Bradshaw, Interaction of tachykinins with phospholipid membranes: a neutron diffraction study, Phys. B Condens. Matter 241 (1997) 1144–1147.
[25] J. Seelig, P.M. Macdonald, Binding of a neuropeptide, substance P, to neutral and negatively charged lipids, Biochemistry 28 (1989) 2490–2496.
[26] C. Kim, S.B. Baek, D.H. Kim, S.C. Lim, H.J. Lee, H.C. Lee, Thermodynamics of partitioning of substance P in isotropic bicelles, J. Pept. Sci. 15 (2009) 353–358.
[27] D.A. Keire, T.G. Fletcher, The conformation of substance P in lipid environments, Biophys. J. 70 (1996) 1716–1727.
[28] S.M. Cowsik, C. Lucke, H. Ruterjans, Lipid-induced conformation of substance P, J. Biomol. Struct. Dyn. 15 (1997) 27–36.
[29] S. Auge, B. Bersch, M. Tropis, A. Milon, Characterization of substance P-membrane interaction by transferred nuclear Overhauser effect, Biopolymers 5 (2000) 297–306.
[30] C. Chatterjee, C. Mukhopadhyay, Melittin–GM1 interaction: a model for a side-by-side complex, Biochem. Biophys. Res. Commun. 292 (2002) 579–585.
[31] A. Gayen, C. Mukhopadhyay, Evidence for effect of GM1 on opioid peptide conformation: NMR study on leucine enkephalin in ganglioside-containing isotropic phospholipid bicelles, Langmuir 24 (2008) 5422–5432.
[32] T.D. Goddard, D.G. Kneller, SPARKY 3, University of California, San Francisco [http://www.csb.yale.edu/userguides/datamanip/sparky/sparky_descrip.html].
[33] R.P.R. Nanga, J.R. Brender, J. Xu, G. Veglia, A. Ramamoorthy, Structure of rat and human islet amyloid polypeptide IAPP1-19 in micelles by NMR spectroscopy, Biochemistry 47 (2008) 12689–12697.
[34] R.P.R. Nanga, J.R. Brender, S. Vivekanandan, N. Popovych, A. Ramamoorthy, NMR structure in a membrane environment reveals putative amyloidogenic regions of the SEVI precursor peptide PAP248–286, J. Am. Chem. Soc. 131 (2009) 17972–17979.
[35] M. Nilsson, M.A. Cornell, A.L. Davis, G.A. Moris, Biexponential fitting of diffusion-ordered NMR data: practicalities and limitations, Anal. Chem. 78 (2006) 3040–3045.
[36] J.F. Wang, J.R. Schnell, J.J. Chou, Amantadine partition and localization in phospholipid membrane: a solution NMR study, Biochem. Biophys. Res. Commun. 324 (2004) 212–217.
[37] I. Marcotte, F. Separovic, M. Auger, S.M. Gagné, A multidimensional 1H NMR investigation of the conformation of methionine-enkephalin in fast-tumbling bicelles, Biophys. J. 86 (2004) 1587–1600.
[38] S. Gaemers, A. Bax, Morphology of three lyotropic liquid crystalline biological NMR media studied by translational diffusion anisotropy, J. Am. Chem. Soc. 123 (2001) 12343–12352.
[39] T.A. Almeida, J. Rojo, P.M. Nieto, F.M. Pinto, M. Hernandez, J.D. Martin, M.L. Candenas, Tachykinins and tachykinin receptors: structure and activity relationships, Curr. Med. Chem. 11 (2004) 2045–2081.
[40] D. Schwieters, J.J. Kuszewski, G.M. Clore, Using Xplor-NIH for NMR molecular structure determination, Prog. NMR Spectrosc. 48 (2006) 47–62.
[41] D. Schwieters, G.M. Clore, The VMD-XPLOR visualization package for NMR structure refinement, J. Magn. Res. 149 (2001) 239–244.
[42] W.L. DeLano, The PyMOL Molecular Graphics System, DeLano Scientific, San Carlos, CA, USA, 2002.
[43] L. Willard, A. Ranjan, H. Zhang, H. Monzavi, R.F. Boyko, B.D. Sykes, D.S. Wishart, VADAR: a web server for quantitative evaluation of protein structure quality, Nucleic Acid Res. 31 (2003) 3316–3319.
[44] N. Fernandez-Fuentes, C.J. Madrid-Aliste, B.J. Rai, J.E. Fajardo, A. Fiser, M4T: a comparative protein structure modeling server, Nucleic Acids Res. 35 (2007) W363–W368.
[45] G.N. Prado, D.F. Mierke, D.F. Mierke, M. Pellegrini, L. Taylor, P. Polgar, Motif mutation of bradykinin B2 receptor second intracellular loop and proximal C terminus is critical for signal transduction, internalization, and resensitization, J. Biol. Chem. 273 (1998) 33548–33555.
[46] C. Rolz, M. Pellegrini, D.F. Mierke, Molecular characterization of the receptor–ligand complex for parathyroid hormone, Biochemistry 38 (1999) 6397–6405.
[47] G. Paterlini, P.S. Portoghese, D.M. Ferguson, Molecular simulation of dynorphin A-(1–10) binding to extracellular loop 2 of the κ-opioid receptor, J. Med. Chem. 40 (1997) 3254–3262.
[48] M. Pelligrini, A.A. Bremer, A.L. Ulfers, N.D. Boyd, D.F. Mierke, Molecular characterization of the Substance P–Neurokinin-1 receptor complex. Development of an experimentally based model, J. Biol. Chem. 276 (2001) 22862–22867.
[49] R. Huey, G.M. Morris, A.J. Olson, D.S. Goodsell, Development of a new type of protease inhibitors, efficacious against FIV and HIV variants, J. Comp. Chem. 28 (2007) 1145–1152.
[50] S. Yao, G.J. Howlett, R.S. Norton, Peptide self-association in aqueous trifluoroethanol monitored by pulsed field gradient NMR diffusion measurements, J. Biomol. NMR 16 (2000) 109–119.
[51] H.R. Mott, P.C. Driscoll, J. Boyd, R.M. Cooke, M.P. Weir, I.D. Campbell, Secondary structure of human interleukin 2 from 3D heteronuclear NMR experiments? Biochemistry 31 (1992) 7741–7744.
[52] G. Wagner, D. Neuhaus, E. Wörgötter, M. Vašák, J.H.R. Kägi, K. Wüthrich, NMR of proteins and nucleic acids, J. Mol. Biol. 187 (1986) 131–135.
[53] N. Hayashi, M. Matsubara, K. Titani, H. Taniguchi, Circular Dichroism and 1H Nuclear Magnetic Resonance studies on the solution and membrane structures of GAP-43 calmodulin-binding domain, J. Biol. Chem. 272 (1997) 7639–7645.
[54] Y. Cong, Z.-Z. Yang, General atom-bond electronegativity equalization method and its application in prediction of charge distributions in polypeptide, Chem. Phys. Lett. 316 (2000) 324–329.
[55] T. Asakura, K. Taoka, M. Demura, M.P. Williamson, The relationship between amide proton chemical shifts and secondary structure in proteins, J. Biomol. NMR 36 (1995) 227–236.
[56] A. Andersson, J. Almqvist, F. Hagn, L. Maler, Diffusion and dynamics of penetratin in different membrane mimicking media, Biochim. Biophys. Acta 1661 (2004) 18–25.
[57] A. Andersson, L. Maler, Motilin–bicelle interactions: membrane position and translational diffusion, FEBS Lett. 545 (2003) 139–143.
[58] A. Andersson, L. Maler, Size and shape of fast-tumbling bicelles as determined by translational diffusion, Langmuir 22 (2006) 2447–2449.
[59] T.C. Wong, X. Gao, The temperature dependence and thermodynamic functions of partitioning of Substance P peptides in dodecylphosphocholine micelles, Biopolymers 45 (1998) 395–403.
[60] Y. Wang, D. Shortle, Residual helical and turn structure in the denatured state of staphylococcal nuclease: analysis of peptide fragments, Fold. Des. 2 (1997) 93–100.
[61] R. Armen, D.O.V. Alonso, V. Daggett, The role of α-, 310-, and π-helix in helix→coil transitions, Protein Sci. 12 (2003) 1145–1157.
[62] J.J. Osterhout Jr., R.L. Baldwin, E.J. York, J.M. Stewart, H.J. Dyson, P.E. Wright, Proton NMR studies of the solution conformations of an analog of the C-peptide of ribonuclease A, Biochemistry 28 (1989) 7059–7064.
[63] A. Wikström, H. Berglund, C. Hambraeus, S.V.D. Berg, T. Härd, Conformational dynamics and molecular recognition: backbone dynamics of estrogen receptor DNA-binding domain, J. Mol. Biol. 289 (1999) 963–979.
[64] N. Zhou, T. Yuan, A.S. Mak, H.J. Vogel, NMR studies of caldesmon–calmodulin interactions, Biochemistry 36 (1997) 2817–2825.
[65] W. Kabch, C. Sander, Dictionary of protein secondary structure: pattern recognition of hydrogen-bonded and geometrical features, Biopolymers 22 (1983) 2577–2637.
[66] C.S. Wu, J.T. Yang, Sequence-dependent conformations of short polypeptides in a hydrophobic environment, Mol. Cell. Biochem. 40 (1981) 109–122.
[67] M. Rueger, M. Bienert, B. Mehlis, K. Gast, D. Zirwar, J. Behlke, Self-association of the neuroregulatory peptide substance P and is C-terminal sequences, Biopolymers 23 (1984) 747–758.
[68] B. Mehlis, M. Rueger, M. Becker, M. Bienert, H. Niedrich, P. Oehme, CD studies of Substance P in aqueous solutions and effects of hydrogen ion concentration, Int. J. Pept. Protein Res. 15 (1980) 20–28.
[69] S.C.J. Sumner, K.S. Gallagher, D.G. Davis, D.G. Covell, R.L. Jemigan, J.A. Ferretti, Conformational analyses of the tachykinins in solutions: Substance P and physalaemin, J. Biomol. Struct. Dyn. 8 (1990) 687–707.
[70] F.J. Corcho, X. Salvatella, J. Canto, E. Giralt, J.J. Perez, Structural analysis of Substance P using molecular dynamics and NMR spectroscopy, J. Pept. Sci. 13 (2007) 728–741.
[71] R.W. Williams, J.L. Weaver, Secondary structure of Substance P bound liposomes in organic solvents and in solution from Raman and CD spectroscopy, J. Biol. Chem. 265 (1990) 2505–2513.
[72] A. Bundi, K. Wuthrich, 1H-nmr parameters of the common amino acid residues measured in aqueous solutions of the linear tetrapeptides H-Gly-Gly-X-Ala-OH, Biopolymers 18 (1979) 285–297.
[73] L. Donghan, K.F.A. Walter, A.-K. Brückner, C. Hilty, S. Becker, C. Griesinger, Bilayer in small bicelles revealed by lipid–protein interactions using NMR spectroscopy, J. Am. Chem. Soc. 130 (2008) 13822–13823.
[74] C. Kang, C.R. Sanders, H.W.D. Van, C.G. Vanoye, R.C. Welch, Structure of KCNE1 and implications for how it modulates the KCNQ1 potassium channel, Biochemistry 49 (2010) 653–655.
[75] M.L. DeMarco, R.J. Woods, J.H. Prestegard, F. Tian, Presentation of membrane-anchored glycosphingolipids determined from molecular dynamics simulations and NMR paramagnetic relaxation rate enhancement, J. Am. Chem. Soc. 132 (2010) 1334–1338.

[76] H.-H. Jang, D.-H. Kim, T. Ahn, C.-H. Yun, Functional and conformational modulation of human cytochrome P450 1B1 by anionic phospholipids, Arch. Biochem. Biophys. 493 (2010) 143–150.
[77] B. Pei, Z.-P. Liu, J.-W. Chen, Ganglioside GM1 biphasically regulates the activity of protein kinase C by the effects on the structure of the lipid bilayer, Chem. Phys. Lipids 114 (2002) 131–138.
[78] C. Heywang, G. Mathe, D. Hess, E. Sackmann, Interaction of GM1 glycolipid in phospholipid monolayers with wheat germ agglutinin: effect of phospholipidic environment and subphase, Chem. Phys. Lipids 113 (2001) 41–53.
[79] C. Yuan, L.J. Johnston, Distribution of ganglioside GM1 in l-α-dipalmitoylphosphatidylcholine/cholesterol monolayers: a model for lipid rafts, Biophys. J. 79 (2000) 2768–2781.
[80] G. Wilkening, T. Linke, G. Uhlhorn-Dierks, K. Sandhoff, Degradation of membrane-bound ganglioside GM1. Simulation by BIS(MONOACYLGLYCERO)PHOSPHATE and the activator proteins SAP-B and GM2-AP*, J. Biol. Chem. 275 (2000) 35814–35819.
[81] H. Ewers, W. Römer, A.E. Smith, GM1 structure determines SV40-induced membrane invagination and infection, Nat. Cell Biol. 12 (2010) 11–18.
[82] A. Andersson, H. Biverstahl, J. Nordin, J. Danielsso, E. Lindahl, L. Maler, The membrane-induced structure of melittin is correlated with fluidity of the lipids, Biochim. Biophys. Acta BBA-Biomembranes 1768 (2007) 115–121.
[83] P.D. Eckford, F.J. Sharom, Interaction of the P-glycoprotein multidrug efflux pump with cholesterol: effects on ATPase activity, drug binding and transport, Biochemistry 47 (2008) 13686–13698.
[84] A. Andersson, L. Mäler, Magnetic resonance investigations of lipid motion in isotropic bicelles, Langmuir 21 (2005) 7702–7709.
[85] P. Brocca, D. Acquotti, S. Sonnino, Nuclear Overhauser effect investigation on GM1 ganglioside containing N-glycolyl-neuraminic acid (II3Neu5GcGgOse4Cer), Glycoconj. J. 13 (1996) 57–62.
[86] P. Brocca, P. Berthault, S. Sonnino, Conformation of the oligosaccharide chain of GM1 ganglioside in a carbohydrate-enriched surface, Biophys. J. 74 (1998) 309–318.
[87] M. Arnold, P. Ringler, A. Brisson, A quantitative electrophoretic migration shift assay for analyzing specific binding of proteins to lipid ligands in vesicles or micelles, Biochim. Biophys. Acta 1233 (1995) 198–204.
[88] O. Convert, H. Duplaa, S. Lavielle, G. Chassaing, Influence of the replacement of amino acid by its D-enantiomer in the sequence of substance P. 2. Conformational analysis by NMR and energy calculations, Neuropeptides 19 (1991) 259–270.
[89] P.I. O'Daniel, J. Zajicek, W. Zhang, Q. Shi, J.F. Fisher, S. Mobashery, Elucidation of the structure of the membrane anchor of penicillin binding protein 5 of *Escherichia coli*, J. Am. Chem. Soc. 132 (2010) 4110–4118.
[90] S.A. Perrine, D.J. Beard, J.K. Young, M.A. Simmons, The role of N-terminal and mid-region residues of Substance P in regulating functional selectivity at the tachykinin NK1 receptor, Eur. J. Pharmacol. 592 (2008) 1–6.
[91] M. Gonzalez, N. Lezcano, M.E. Celis, G.D. Fidelio, Interaction of alpha-MSH and substance P with interfaces containing gangliosides, Peptides 17 (1996) 269–274.
[92] S.V. Dvinskikh, U.H.N. Dürr, K. Yamamoto, A. Ramamoorthy, High-resolution 2D NMR spectroscopy of bicelles to measure the membrane interaction of ligands, J. Am. Chem. Soc. 129 (2007) 794–802.
[93] F. Hanakam, G. Gerisch, S. Lotz, T. Alt, A. Seelig, Binding of substance P agonists to lipid membranes and to the neurokinin-1 receptor, Biochemistry 35 (1996) 4365–4374.
[94] N.D. Boyd, R. Kage, J.J. Dumas, J.E. Krause, S.E. Leeman, The peptide binding site of the substance P (NK-1) receptor localized by a photoreactive analogue of substance P: presence of a disulfide bond, Proc. Natl. Acad. Sci. U. S. A. 93 (1996) 433–437.